Ambio
https://doi.org/10.1007/s13280-024-02042-3

KUNGL. VETENSKAPS-AKADEMIEN
THE ROYAL SWEDISH ACADEMY OF SCIENCES

RESEARCH ARTICLE

Dynamics of ecosystem services and nonlinear responses to increased anthropogenic pressure

Chenghao Liu, Yaobin Liu, Biagio Fernando Giannetti, Cecília Maria Villas Bôas de Almeida, Guoen Wei, Fábio Sevegnani, Xiaolu Yan

Received: 24 February 2024 / Revised: 30 April 2024 / Accepted: 20 May 2024

Abstract Escalating global human activities elicit diverse ecosystem service responses, yet understanding remains limited. This study establishes a framework to clarify these responses, focusing on the Yangtze River Economic Belt in China. Analyzing 2000–2020 data, it calculates ecosystem service economic value and human footprint index. It introduces the ecosystem services response index and comprehensive responsiveness index to assess response characteristics and intensity to anthropogenic pressures. Results show a fluctuating decline in ecosystem services and an increase in anthropogenic pressures. There is a nonlinear relationship: ecosystem services decline with rising pressures, following a U-shaped trend. Notably, nonurban agglomerations experience more significant ecosystem service evolution than urban agglomerations due to differing environmental conditions. This highlights regional disparities in human activity impacts on ecosystems, crucial for planning.

Keywords Comparative analysis · Ecosystem services · Human footprint index · Nonlinear · Regional disparities

INTRODUCTION

Ecosystem services (ES) play a crucial role in supporting economic and social frameworks (IPBES 2019). The estimation of the economic value of ecosystem services (ESV) serves as a foundational reference point for determining the magnitude of ES contributions (Costanza et al. 2014). However, as the scale and scope of human activities continue to expand, ecosystems face severe degradation, destruction, and the potential for collapse, thereby jeopardizing these invaluable ESs and triggering cascading effects on human well-being (Luo and Zhang 2022; Smith et al. 2022). This phenomenon is not only pronounced at the local level, but also manifests as a global challenge (Giannetti et al. 2018; Marques et al. 2019; Keyes et al. 2021). This underscores the imperative for in-depth investigations into the responses of ES to heightened anthropogenic pressures, facilitating effective coordination of human activities.

Currently, research on the impact of human activities on ES can be categorized into two main types. Firstly, one category focuses on confirming whether human activities have a discernible impact on ES and the direction and magnitude of such impacts. These studies typically employ statistical analysis and scenario simulation methods to validate the relationships between specific anthropogenic factors (e.g., urbanization, agricultural expansion, and mining activities) and ES (Souza et al. 2021; Kong et al. 2023; Pham and Lin 2023). Additionally, some studies explore variations in the impact of different anthropogenic factors on ES (Lu et al. 2021; Yang et al. 2022b). However, it is noteworthy that these studies often limit themselves to descriptive analyses of the impacts and do not delve deeply into uncovering the underlying mechanisms driving these effects.

The second category of studies underscores human activities impact ES through complex mechanisms. Due to the uneven distribution of social–ecological resources, the spatial heterogeneity of ES is widely confirmed (Chung et al. 2021; Chen et al. 2022; Filho et al. 2022). Furthermore, the anthropogenic drivers behind the evolution of ES

Supplementary Information The online version contains supplementary material available at https://doi.org/10.1007/s13280-024-02042-3.

exhibit evident spatial non-stationarity (Han et al. 2020; Wang et al. 2022). For instance, Yu et al. (2023) explored the scale effects and spatial heterogeneity of the impact of urban compact factors, such as population density in rapidly urbanizing metropolitan areas, on ES. Additionally, due to the flow of materials, human movements, and other dynamics, the influence of human activities on ES extends beyond local boundaries (Shi et al. 2022). For example, Chen and Chi (2022) found spatial spillover effects of urbanization on ES. It is noteworthy that human activities do not always directly impact ES; rather, they may indirectly influence ES through various factors and pathways (Li et al. 2022). The aforementioned processes often focus on individual regions, with relatively less attention to differences between regions at different stages of development. Furthermore, despite enriching the understanding of the mechanisms through which human activities influence ES, these studies often emphasize linear relationships, while potential nonlinear relationships remain inadequately addressed.

In general, the impact of human activities on ES has been widely acknowledged. Ecosystems possess highly complex and dynamic characteristics, meaning that this impact often entails not merely a simple linear relationship but rather a more intricate nonlinear association. This implies that as the pressure exerted by human activities increases, the direction and magnitude of ES change correspondingly shift. In other words, when external conditions (e.g., anthropogenic pressure) exceed certain tipping points, the state of ecosystems may undergo catastrophic shifts (Scheffer et al. 2001; Kéfi et al. 2022). Indeed, such catastrophic shifts have been extensively discussed in numerous studies (Mumby et al. 2007; Carpenter et al. 2011; van Belzen et al. 2017). However, it remains unclear whether a nonlinear relationship exists between anthropogenic pressure and ES. Applying the concepts of nonlinearity and tipping points to the relationship between anthropogenic pressure and ES could offer vital tools for ecosystem management, enabling early warning of potential issues.

To address these questions, this study, using 1071 districts/counties in the Yangtze River Economic Belt (YREB) in China as an example, has preliminarily established a conceptual framework elucidating the impact of anthropogenic pressures on ES. Integrating remote sensing, socioeconomic, and ecological data, this study quantitatively analyzes the levels of anthropogenic pressure and ES by calculating the human footprint index (HFI) and ESV. Subsequently, the concept of elasticity was applied to construct the ES response index and comprehensive ES responsiveness index, aiming to describe the characteristics and extent of ES response to increasing anthropogenic pressure and to validate the potential nonlinear relationship between the two. Finally, comparative analysis was employed to reveal regional variations in ES responses to anthropogenic pressures at different stages of development and locations, providing a basis for formulating differentiated management strategies.

MATERIALS AND METHODS

Study area

The YREB, characterized by the world's third-longest river, the Yangtze River, serves as the principal waterway, spanning the eastern, central, and western regions of China (Fig. 1). It boasts abundant water resources and diverse ecosystems. The favorable resource conditions have supported its economic development. Along the upstream, midstream, and downstream of the Yangtze River, three major urban agglomerations (UA) have sequentially emerged: The Chengdu-Chongqing urban agglomeration (C&C), the middle reaches of the Yangtze River urban agglomeration (MRYR), and the Yangtze River Delta urban agglomeration (YRD). According to the annual report on the development of the Yangtze River Economic Belt (2019–2020), in 2019, these three major UAs collectively housed approximately 28.4% of China's population and contributed to around 36.6% of the national GDP (Wang et al. 2021). Simultaneously, areas outside these three UAs within the YREB (referred to as non-UA) played a crucial supporting role in economic development. However, unrestricted resource utilization has made the YREB an ecological hotspot of concern. In response, the Chinese government has outlined a positioning strategy of comprehensive protection and restrained development to promote the high-quality development of the YREB. Nevertheless, challenges to social-ecological sustainability persist and demand urgent resolution.

Analysis framework

This study, based on the "Pressure (P)–State (S)–Impact (I)–Response (R)" framework (Fig. 2), aims to deepen the exploration of ES response mechanisms to anthropogenic pressures. The study also proposes refined and practical management strategies, striving to safeguard ecological environments while pursuing human well-being. Human efforts towards enhancing well-being invariably impose pressures on the environment across various dimensions (Pires de Souza Araujo et al. 2021), including production, consumption, and circulation. Under the influence of these pressures, spatially diverse variations in the status of

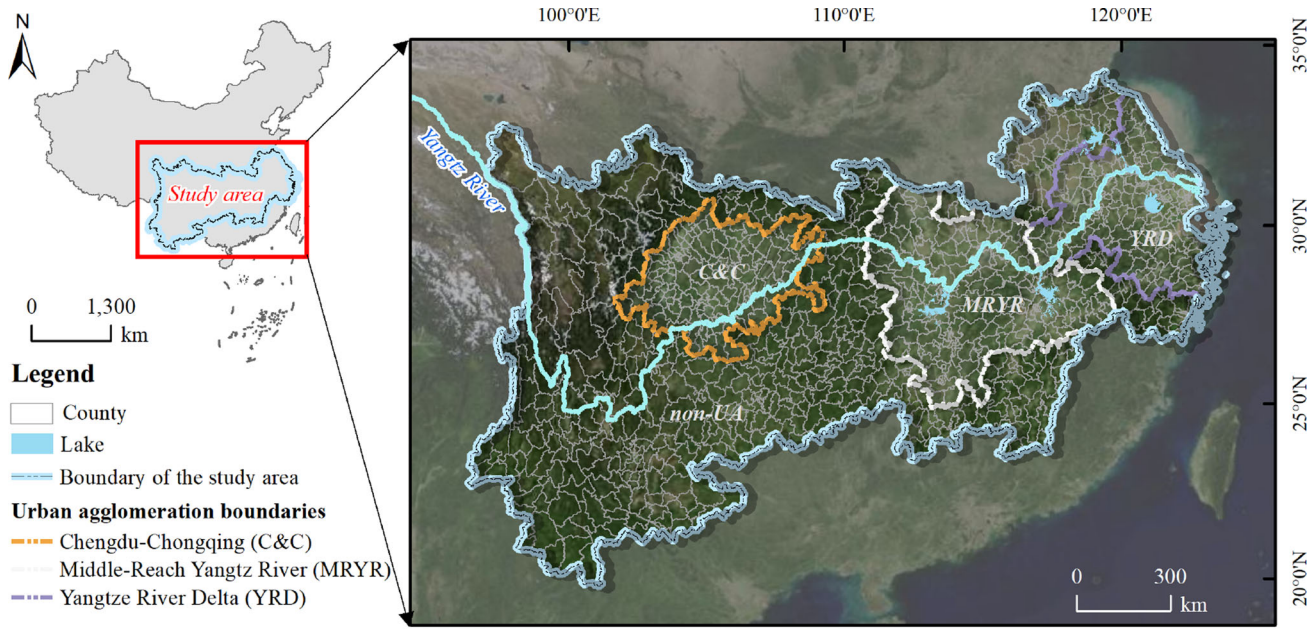

Fig. 1 Study area. Note: The specific county names are displayed in Figure S1

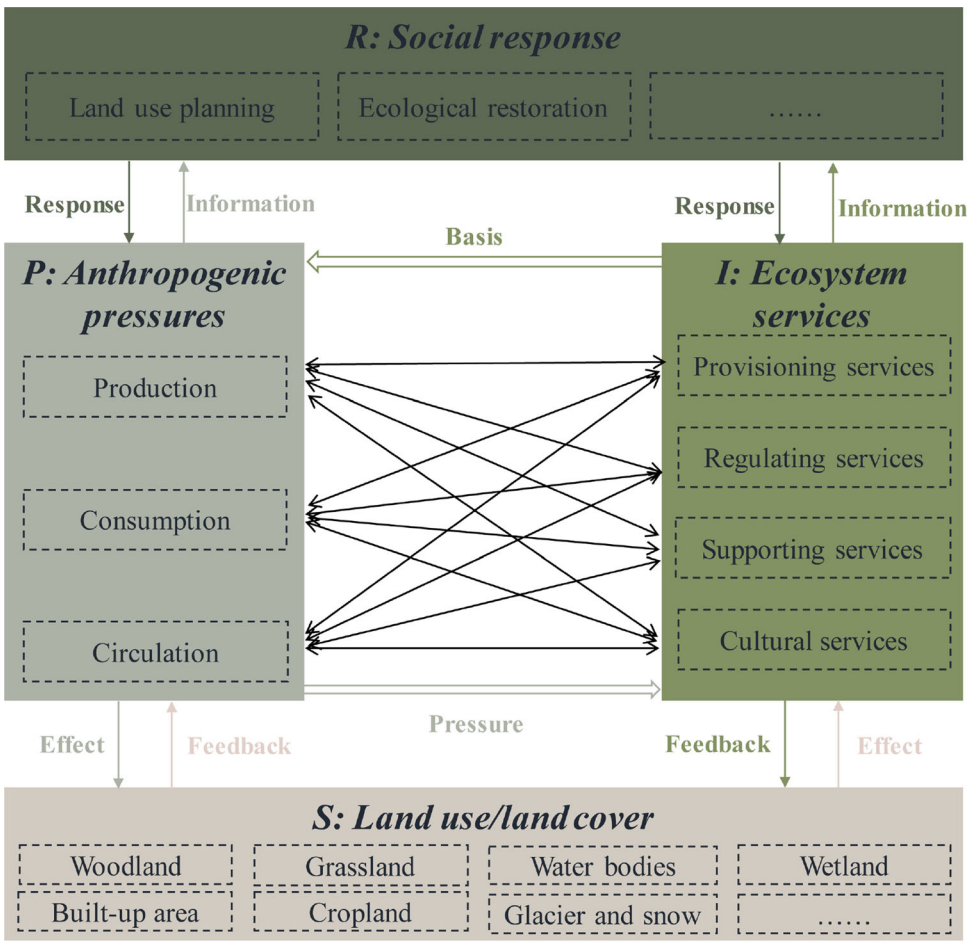

Fig. 2 Analysis framework

ecosystems occur, particularly concerning land use/land cover (LULC) change (Zalles et al. 2023). These alterations directly impact the structure and functionality of ecosystems, subsequently influencing their capacity to provide diverse products and services for humanity (Maestre et al. 2022). Indeed, the manner and intensity with which ES responds to anthropogenic pressures embody outcomes of socio-ecological interactions. Such responses, in turn, provide feedback to the societal systems. Furthermore, society, through effective land use planning (Nijhum et al. 2021), ecological restoration measures (Yang et al. 2022a, b), and similar strategies, seeks to mitigate anthropogenic pressures, thereby attaining harmonious co-development of humans and nature.

Date sources

The data used in this study are as follows: (1) Three-period LULC data for 2000, 2010, and 2020 were derived from the Resource and Environmental Science Data Platform, Chinese Academy of Sciences (https://www.resdc.cn/). (2) Three-period normalized vegetation index data were acquired from MOD13Q1 dataset of U.S. Geological Survey (http://glovis.usgs.gov/). (3) Meteorological data for 2000, 2010, and 2020 were obtained from the China Meteorological Data Service Center (http://data.cma.cn/). (4) Three-period population density data were obtained from the WorldPOP dataset (https://hub.worldpop.org/). (5) 2000–2020 nighttime light data were acquired from the National Oceanic and Atmospheric Administration (https://www.ngdc.noaa.gov/) after a series of processing culminating in a curve fit to combine DMSP/OLS and NPP/VIIRS datasets were matched. (6) Slope and slope direction data were derived from Geospatial Data Cloud, Chinese Academy of Sciences (http://www.gscloud.cn). (7) Soil data were obtained from China soil map based Harmonized World Soil Database, National Tibetan Plateau/Third Pole Environment Data Center (http://data.tpdc.ac.cn). (8) Road and railway data for 2000 and 2009 were obtained from Geographic Data Sharing Infrastructure, College of Urban and Environmental Science, Peking University (http://geodata.pku.edu.cn), and the road distribution pattern for 2009 was substituted for that of 2010 due to the availability of data and the proximity of years. The data for 2020 were derived from the Resource and Environmental Science Data Platform, Chinese Academy of Sciences (https://www.resdc.cn/). (9) Shipping waterway data for 2000, 2010, and 2015 were obtained from the National Earth System Science Data Center (http://www.geodata.cn), with 2015 waterways replacing 2020 given data availability and proximity of the years. (10) 2000–2020 socioeconomic data were derived from the Statistical Yearbook.

Methods

Analyzing anthropogenic pressure

The HFI serves as a quantification of anthropogenic pressure on the environment. Proposed by Sanderson et al. (2002), the HFI has gained widespread application and expansion across various global scales (Venter et al. 2016; Correa Ayram et al. 2017; Wan et al. 2018). In alignment with the specifics of the study area, this research incorporates a selection of five distinct variables to represent anthropogenic pressure within production, consumption, and circulation. Further subdivision yields nine proxy indicators (or pressure sources) as shown in Table 1. Each indicator corresponds to a distinct layer, and the final HFI is computed utilizing Theobald's (2013) approach (Eq. 1) which overcomes possible correlations between the layers. This approach posits that locations experiencing multifaceted pressure sources exhibit greater anthropogenic disturbance compared to those with singular pressure sources. The resultant HFI dataset is generated at a spatial resolution of 1 km^2.

$$\mathrm{HFI}_i = 1 - \prod_{j=1}^{k} \left(1 - h_j\right), \tag{1}$$

where HFI_i represents the HFI value for the ith unit, h_j denotes the impact score for the jth indicator, and k signifies the number of data layers.

Calculation of ESV

The equivalent standard value method is employed for the estimation of ESV. The China unit area ESV equivalent factor table, constructed by Xie et al. (2015), reflects the annual average state of ESV in China. Building upon this foundation and acknowledging the potential inaccuracies in characterizing regional features through national parameter tables, as well as the dynamic nature of ESV, the table was adapted based on dynamic material quantities, leading to the estimation of ESV for YREB. The process is outlined as follows:

(1) Construction of the dynamic equivalent factor table: Rainfall is used to adjust water resource supply and hydrological regulation, soil retention is corrected based on soil retention simulated using the RUSLE model, and other ESs are adjusted according to Net Primary Productivity, simulated using the CASA model constructed by Zhu et al. (2005). By iteratively applying the above methods, yearly adjustments are made to achieve dynamic ESV estimation (Formula 2).

$$E_{ij} = e_{ij}\frac{\overline{n}}{\overline{N}}, \tag{2}$$

Table 1 The influence scores of data layers

Dimension	Variable	Proxy	Human influence score
Production	Land	Land use	The production activities of YREB manifest on land cover categories such as built-up area, cropland, garden land, and grassland, with corresponding assigned values of 1, 0.7, 0.4, and 0.4, respectively, as established by Sanderson et al. (2002)
	Energy consumption	Night time light	Building upon the methodology of Venter et al. (2016), the calibrated DMSP-OLS and NPP-VIIRS datasets were processed. For grid cells within these datasets where the nighttime light digital number (DN) value equaled 0, a value of 0 was assigned. For all other cases, a quantile-based classification approach was employed, resulting in ten classes ranging from 0.1 to 1 on the impact score scale. Subsequently, using the binning thresholds established from the year 2000 dataset, the data from the years 2010 and 2020 were transformed to a comparable scale of 0.1–1
Consumption	Population	Population density	The logarithmic equation assignment method was employed (Venter et al. 2016) $H_{\text{score}} = \frac{\log(p+1)}{\log(p_{\max}+1)}$, where p represents population density, and $p_{\max}$ denotes the maximum population density within the study area
Circulation	Distance from road	Major highway	Assign a score of 1 and decay linearly, assigning a score of 0 for values beyond the maximum impact distance $H_{\text{score}} = 1 - \left(\frac{d}{d_{\max}}\right)$ where d represents human influence distance, $d_{\max}$ signifies the maximum distance of impact with 3 km
		Railway Shipping waterway	Shipping lanes were assigned a score of 0.4 (Venter et al. 2016), while others were assigned a score of 1, decaying exponentially. Values were set to 0 beyond the maximum impact distance $H_{\text{score}} = \exp\left[-\left(\frac{2.99}{d_{\max}}\right)d\right]$ where d represents the human influence distance, and the maximum influence distances $d_{\max}$ are as follows. Railways: 4 km, shipping waterway: 15 km, urban land: 10 km, industrial land: 6 km, rural settlements: 5 km
	Distance from the built-up area	Urban land Industrial land Rural settlements	

where E_{ij} represents the adjusted equivalent factor for the ith LULC's jth ES, e is the initial equivalent factor, and $\overline{n}$, and $\overline{N}$ denote the mean value of the corrective factors in YREB and China, respectively.

(2) Computation of the economic value of 1 standard unit equivalent factor: This economic value corresponds to 1/7th of the average market value of cereal crops for that year. Recognizing the influence of technological and market factors on cereal crop production and prices, this study takes the average economic value from 2000 to 2020 as the standard. Based on the aforementioned two steps, ESV is estimated (Formula 4).

$$D = \frac{1}{21}\sum_{n=2000}^{2020}\frac{1}{7}\times\frac{P_n}{Q_n \times I_n} \tag{3}$$

$$\text{ESV} = \sum_{i=1}^{7}\sum_{j=1}^{11} S_i \times D \times E_{ij}, \tag{4}$$

where D represents the economic value (in USD/ha) of one standardized unit of equivalent factor, P_n is the yearly crop output (in USD) for the nth year, with the average exchange rate between the CNY and the USD for the years 2000–2020. Q_n represents the cultivated area (in ha) for food crops in a given year, I_n signifies the price index to convert crop output to 2000 constant prices, S_i denotes the ith LULC's area (in ha), E_{ij} represents the adjusted equivalent factor for the ith LULC's jth ES.

Pearson correlation analysis

To investigate the relationship between anthropogenic pressure and ES, this study employed the Pearson correlation analysis method. By calculating the Pearson correlation coefficient (Formula 5), it was determined whether there was a certain degree of correlation between anthropogenic pressure and ES, as well as the direction and strength of this correlation. In essence, this analysis method provides results ranging from -1 to 1, where -1 indicates a perfect negative correlation, 1 indicates a perfect positive correlation, and 0 indicates no linear relationship.

$$r = \frac{\sum (x - \bar{x})(y - \bar{y})}{\sqrt{\sum (x - \bar{x})^2 \sum (y - \bar{y})^2}}, \quad (5)$$

where x and y represent the values of the HFI and ESV, while $\bar{x}$ and $\bar{y}$ represent the respective means of HFI and ESV values.

Ecosystem services response indexes

Current research indicates that anthropogenic pressure affects ES (Qi et al. 2020; Yongxiu et al. 2020). This relationship is represented in this study by the function ESV = f(HFI). To quantitatively, measure the impact of anthropogenic pressure on ES, this study defines the ES response index as the change in ESV for each unit increase in HFI. This index is employed to describe the response characteristics and trends of ES to increasing anthropogenic pressure.

$$I = d(\text{ESV})/d(\text{HFI}), \quad (6)$$

where I is the ES response index, d(ESV)/d(HFI) is the derivative of ESV concerning HFI. When $I > 0$, it suggests that the expansion of anthropogenic pressures promotes an increase in ES levels. When $I < 0$, it signifies a negative response of ES to the expansion of anthropogenic pressures. When $I = 0$, ES changes may exhibit no response to the increase in anthropogenic pressures.

To further compare the overall characteristics of how ES responds to anthropogenic pressure in different regions, building upon Eq. 6, this study establishes the comprehensive ES responsiveness index. This index characterizes the degree of response of regional ES to increasing anthropogenic pressure over a certain period. The higher the value, the greater the change in ES caused by the expansion of anthropogenic pressure, which means that the ES is more sensitive to anthropogenic pressure. On the contrary, the lower the value, the smaller the change in ES caused by artificial pressure expansion.

$$R = \frac{1}{n} \sum_{i=1}^{n} |I_i|, \quad (7)$$

where R is the comprehensive ES responsiveness index, n is the number of counties within a region, and I_i represents the ES response index of the ith county within that region.

Random forest model

Random forest models, with their resistance to overfitting and high accuracy, are widely used in feature importance assessment (Peng et al. 2021; Zhang et al. 2021). In this study, 80% of the samples were used as the training set, and 20% of the samples were reserved for accuracy validation. The mean decrease accuracy method of the model was used to evaluate the importance of anthropogenic stressors affecting ES response, where a higher value indicates greater importance of the variable. This method assesses the impact of features on model accuracy by shuffling (permuting) the features; the larger the change in accuracy, the greater the contribution of the feature to the model.

RESULTS

Changes in ESV over time

In terms of total value, the ESV of YREB decreased from 679.85 thousand million USD in 2000 to 657.09 thousand million USD in 2010, and then rose to 673.53 thousand million USD in 2020, resulting in an overall decrease of 0.93% (Table 2). When examining ESV across different ecosystem types, forest ecosystems had the highest ESV, accounting for approximately 55% of the total ESV, followed by aquatic and grassland ecosystems at approximately 24% and 12%, respectively. Looking at the dynamics over the 20 years, there is a noticeable shift around the year 2010, with significant changes observed in the first decade. ESV for water bodies, glaciers and snow, and wetland ecosystems all showed varying degrees of increase, while other ecosystems displayed varying degrees of decline. Although ESV for forest, grassland, and unused land ecosystems experienced slight increases from 2010 to 2020, they were unable to offset the reductions observed from 2000 to 2010. Meanwhile, ESV for cropland continued to decline. This highlights that LULC change has had a discernible impact on the regional ESV.

In terms of ESV per unit area during the study period, the UA consistently exceeded the non-UA and the YREB (Fig. 3a). The ESV per unit area ranking of the three UAs was MRYR > YRD > C&C. Over the span of 20 years, ESV changes in these regions exhibited a similar pattern, characterized by an initial decrease followed by an upward trend. Notably, apart from the YRD, all regions experienced a smaller magnitude of increase compared to the preceding decrease (Fig. 3b). Additionally, ESV fluctuations in the non-UA were more pronounced compared to the UA. Regarding spatial changes, from 2000 to 2010, approximately 88% of counties in the study area witnessed varying degrees of ESV decline. The steepest declines ($-$ 87.10% $\sim$ $-$ 6.67%) were predominantly observed in

Table 2 ESV for different ecosystems (in thousand million USD)

Land use/land cover	Year			Change rate (%)		
	2000	2010	2020	2000–2010	2010–2020	2000–2020
Cropland	49.83	45.26	45.43	− 9.16	0.37	− 8.83
Woodland	376.57	359.06	365.23	− 4.65	1.72	− 3.01
Grassland	84.07	76.44	78.02	− 9.08	2.07	− 7.20
Water bodies	162.94	169.48	177.74	4.02	4.87	9.08
Glacier and snow	0.21	0.23	0.24	8.27	2.08	10.53
Wetland	6.16	6.56	6.81	6.46	3.80	10.51
Unused land	0.07	0.06	0.06	− 11.92	1.19	− 10.87
Total	679.85	657.09	673.53	− 3.35	2.50	− 0.93

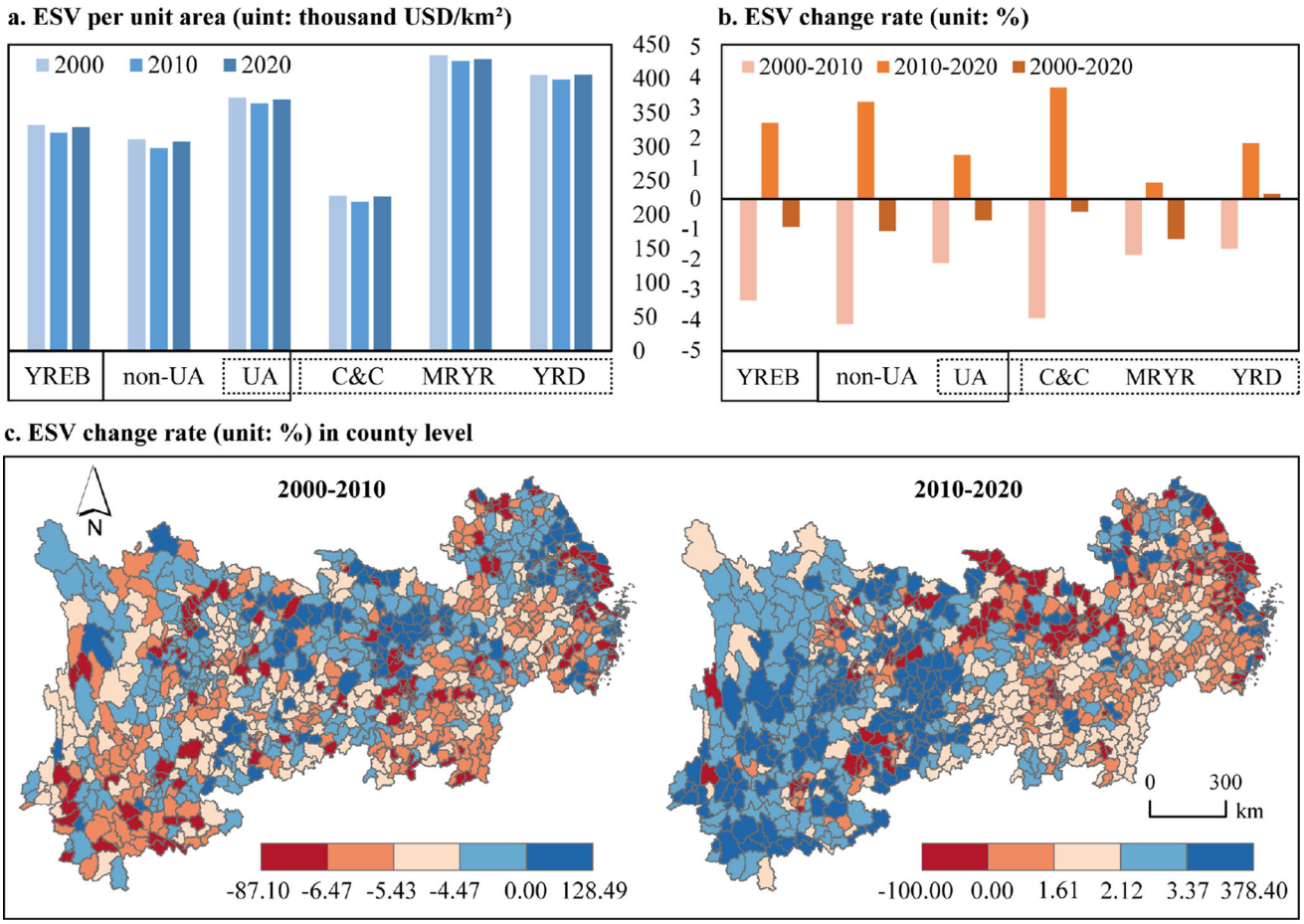

Fig. 3 ESV per unit area (**a**), the change rate of ESV (**b**), and maps depicting the county-level ESV change rate (**c**) for the YREB from 2000 to 2020

economically developed counties. Conversely, some counties experienced modest ESV increases, often attributed to the presence of extensive water bodies. From 2010 to 2020, approximately 81% of counties in the study area saw ESV increases, with the western part of the study area showing relatively larger ESV gains.

Characteristics of anthropogenic pressure and its relationship to ES

Changes in anthropogenic pressure over time

From 2000 to 2020, the HFI in the YREB exhibited a consistent upward trend (Fig. 4), rising from 0.59 in 2000

to 0.60 in 2010, and further increasing to 0.63 by 2020, representing an approximately 6.78% increase. This indicates a continuous expansion of anthropogenic pressure pressures in the YREB since 2000, particularly during the period from 2010 to 2020. One possible explanation for this trend is the rapid development of infrastructure in the study area after 2010. Furthermore, these anthropogenic pressures exhibit significant spatial variation. Counties with the highest pressures (HFI > 0.90) are primarily concentrated in the northeastern part of the study area, which is characterized by relatively higher economic development. Conversely, counties with the lowest pressures (HFI < 0.30) are mainly clustered in the western region, characterized by a terrain of plateaus and mountains.

When examining different subregions, the HFI for the UA is notably higher than that for the YREB and the non-UA. Within the UAs, the HFI means follow the sequence YRD > C&C > MRYR (Fig. 4d). From 2000 to 2020, anthropogenic pressures increased to varying degrees in different regions, with high HFI values expanding outward, particularly in the C&C and the northeastern part of the study area. Moreover, the differences in anthropogenic pressures within the three UAs have been steadily decreasing over time.

Correlation analysis between anthropogenic pressure and ES

Table 3 reveals a significant negative correlation between anthropogenic stress and ES, indicating that ESV tends to decrease with an increase in local anthropogenic pressure. From 2000 to 2020, the overall negative correlation in the YREB slightly increased, changing from − 0.74 in 2000 to − 0.75 in 2020. Furthermore, there are varying degrees of negative correlations between anthropogenic pressure and ES across different geographic regions. Particularly, the non-UA exhibits a stronger negative correlation compared to the UA. Among the UAs, the C&C shows the most significant negative correlation. Notably, during the period from 2010 to 2020, the MRYR negative correlation strength surpasses that of the YRD. These variations in

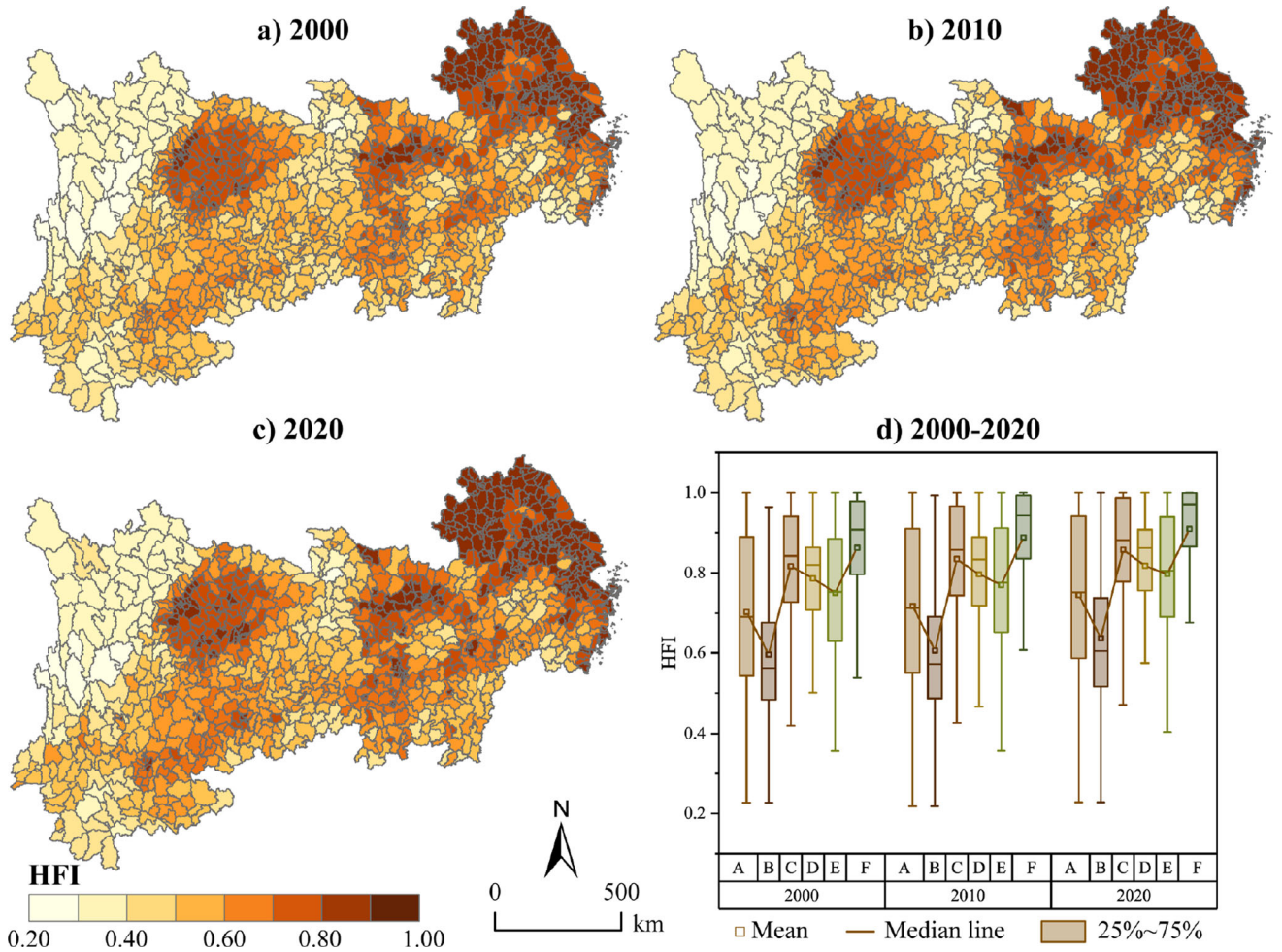

Fig. 4 HFI maps (**a**–**c**) and box plots (**d**) of the YREB from 2000 to 2020. A, YREB. B

correlations can be attributed to the different developmental statuses and characteristics of each region.

Response of ES to increased anthropogenic pressures

Figure 5a illustrates that in the YREB, the ES response index consistently exhibits negative values, indicating a decline in ESV with increasing anthropogenic pressure. As HFI increases, the absolute value of the ES response index decreases, suggesting that the adaptive capacity of the YREB ecosystem itself slows down the decline in ESV. However, when HFI exceeds 0.73, the absolute value of the ES response index begins to gradually increase, which may imply that the ES of YREB is facing irreversible risks.

The fitting results indicate that there are diverse forms of response functions (Fig. 5), suggesting spatial heterogeneity in ES changes in the face of increasing anthropogenic pressure. Further comparison of the ES response index in different regions of YREB reveals that non-UA exhibits patterns similar to the study area (Fig. 5b), and when HFI exceeds 0.76, the ES of non-UA may face irreversible risks. Conversely, UA exhibits different characteristics: With increasing anthropogenic pressure, the ES response index in UA gradually transitions from positive values to negative values, with the negative values continuously decreasing (Fig. 5c). This suggests that the initial increase in anthropogenic pressure leads to an increase in ESV, but when HFI exceeds 0.39, ESV begins to decrease, with the reduction rate gradually increasing. It can be observed that in the face of increasing anthropogenic pressure, the ES of non-UA is more sensitive compared to that of UA, which is also shown by Table 4.

For different UAs in YREB, the Comprehensive ES Response Index shows a ranking of YRD > MRYR > C&C (Table 4), indicating that YRD is relatively more sensitive to increasing anthropogenic pressure, followed by MRYR, while the ES change in C&C is minimal. Specifically, the ES level in YRD continues to decline under increasing anthropogenic pressure (Fig. 5d). Due to its ecosystem's adaptive capacity, the extent of the decline in ESV is reduced. However, when the level of anthropogenic pressure exceeds 0.73, the ES of YRD may face collapse risks. MRYR exhibits similar patterns with UA; when HFI exceeds 0.46, ESV transitions from an increase to a continuous decrease, with the rate of decline showing an increasing trend (Fig. 5e). In comparison, the ES response pattern in C&C is more complex. Its ES response index shows a U-shaped trend, and when HFI exceeds 0.41, there is a shift from positive to negative ES response direction, resulting in an increase followed by a decrease in the magnitude of ESV decline (Fig. 5f).

DISCUSSION

Nonlinear responses of ES to increased anthropogenic pressures

The findings of this study reveal the dynamic and heterogeneous response of ES to increased anthropogenic pressures. The ecosystem comprises biotic and abiotic components, exhibiting complex interactions and feedback mechanisms (Geary et al. 2020). For instance, human activities such as urbanization and agricultural expansion lead to extensive loss and degradation of habitats (Fig. 6). Initially, some species may adapt to the new environmental conditions, but as habitat degradation intensifies, a tipping point may be reached, resulting in an accelerated extinction rate and posing a severe threat to ecosystem stability (Banks-Leite et al. 2020; Ma et al. 2023). This is consistent with the findings of the study, which indicate a deceleration followed by an enhancement in the rate of ESV decline despite the increase in anthropogenic pressure.

Further analysis of these phenomena can be elucidated using the ecological resilience theory. In the early stages, ecosystems exhibit resistance, adaptation, and recovery capabilities in response to anthropogenic pressure, thereby

Table 3 Pearson correlation coefficient for HFI-ESV in YREB and its subregions

Name	2000	2010	2020
YREB	− 0.74**	− 0.74**	− 0.75**
Non-UA	− 0.63**	− 0.61**	− 0.63**
UA	− 0.54**	− 0.51**	− 0.52**
YRD	− 0.54**	− 0.50**	− 0.52**
MRYR	− 0.52**	− 0.51**	− 0.54**
C&C	− 0.73**	− 0.73**	− 0.72**

**Correlation is significant at the 0.01 level (2-tailed)

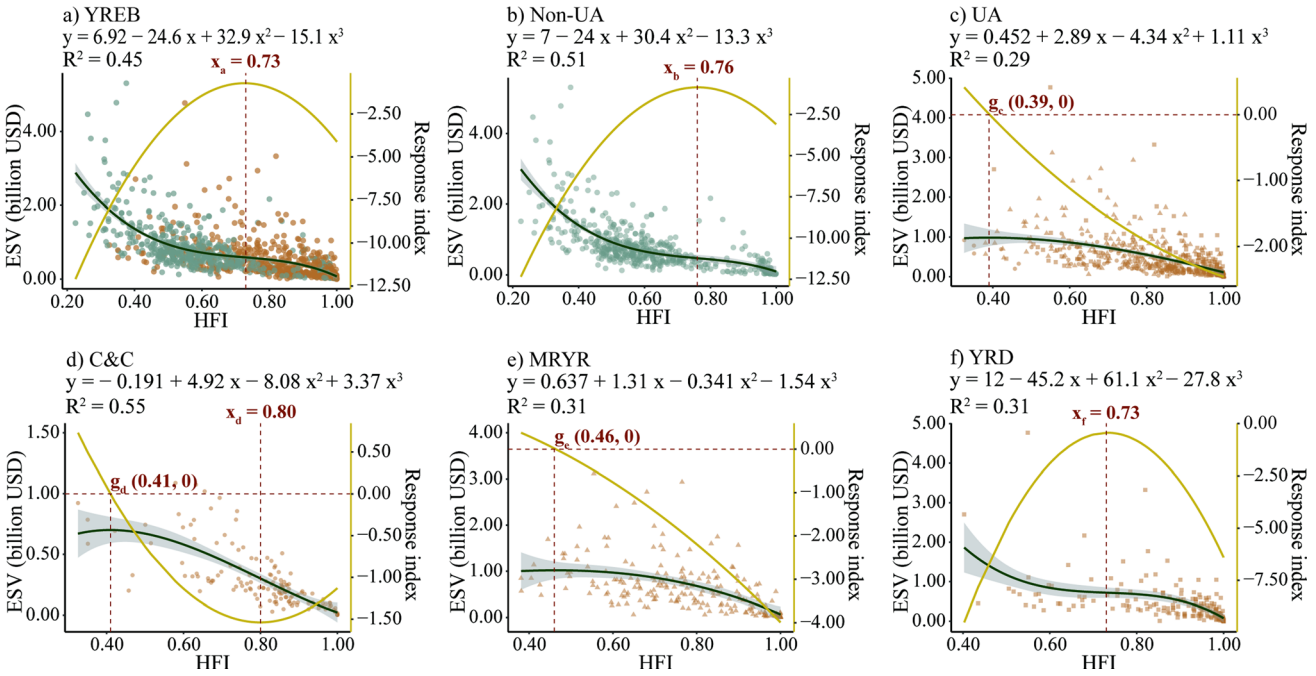

Fig. 5 Fitting results (green line) for ESV and HFI, along with the variation in ES response index (yellow line). Notably, the larger the absolute value of the index, the more evident the ESV change, indicating a heightened sensitivity of ecosystem services to increased anthropogenic pressure. The equations and R^2 in the inset represent the ESV and HFI best-fit models and their goodness-of-fit. The intersection of the red dashed line and the yellow solid line in the inset represents the anthropogenic pressure tipping point. For example, when the HFI exceeds point g, an increase in anthropogenic pressures leads to a change in ES from increasing to decreasing (or vice versa). When the HFI exceeds the dashed line $x = c$ (where c represents a constant), an increase in anthropogenic pressures can amplify or mitigate the extent of ES change

Table 4 Regional comparison of the comprehensive ES responsiveness index

Name	YREB	Non-UA	UA	C&C	MRYR	YRD
Value	2.50	3.08	1.92	1.36	2.11	3.94

slowing down the decline in ESV. However, as anthropogenic pressure intensifies and surpasses a certain tipping point (e.g., H_2 in Fig. 6), it may trigger internal threshold effects within the ecosystem, leading to a sharp decline in ESV. This discovery provides profound insights, emphasizing the delicate and crucial balance between ecosystem resilience and stability under anthropogenic pressure. Therefore, considering the dynamic response of ecosystems to varying degrees of pressure is key to understanding the nonlinear response of ES and facilitates better planning and management of human activities impacting the natural environment.

Reasons for regional differences in nonlinear responses of ES to increased anthropogenic pressures

Environmental conditions influence the ES response

This study reveals significant differences in the response of the ES to anthropogenic pressures in UA and non-UA. ES changes in non-UA are more sensitive compared to UA (Fig. 5b, c). This suggests that, despite often facing higher levels of urbanization and anthropogenic pressures, UA can, in some cases, maintain relatively stable ES. This contrasts with findings from a study conducted by Pan et al. (2023) in China, primarily due to differing environmental conditions in the study areas.

The UA heavily relies on water resources due to the development of its lake and river systems. These geographical features may influence the structure and function of ecosystems, leading to distinct responses to anthropogenic pressures compared to other regions. This is shown in Fig. S2, where the water body has the largest supply capacity in ESV for UA. Forests had the largest ESV per unit area in non-UA. Furthermore, aquatic ecosystems and forest ecosystems exhibit different vulnerability characteristics. Aquatic ecosystems are susceptible to factors such as pollution, water level fluctuations, and water quality changes (Grant et al. 2021; Nava et al. 2023), while forest ecosystems are more sensitive to land use changes,

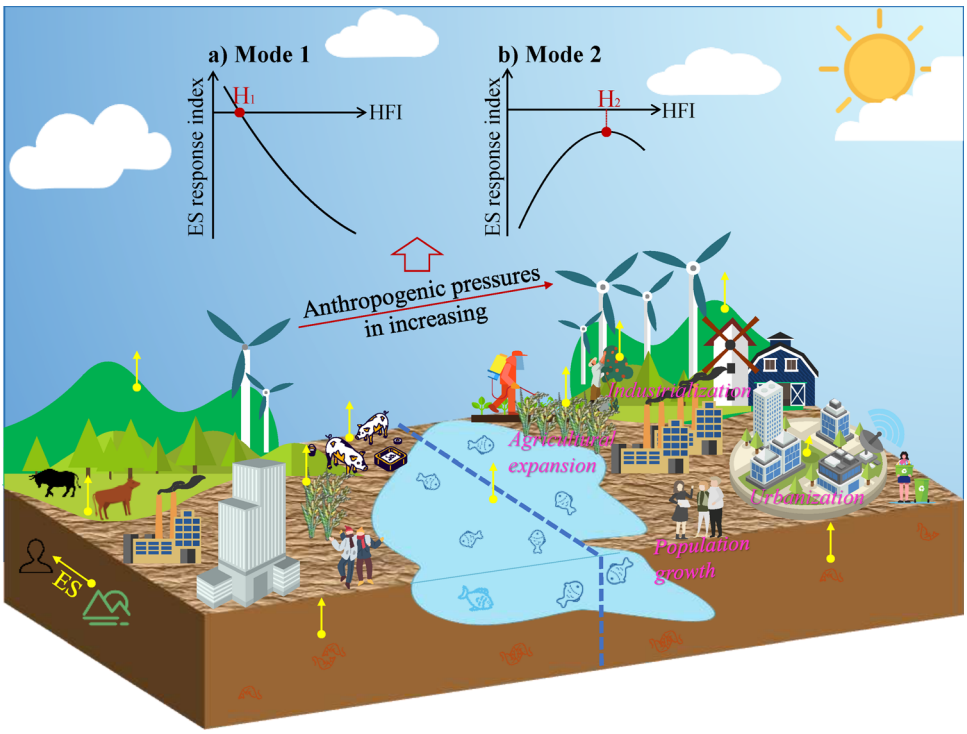

Fig. 6 The process of increasing anthropogenic pressure and the mode of ES response

deforestation, and biodiversity loss (Buchadas et al. 2022; Thaweepworadej and Evans 2022). These differences may result in a relatively smaller decline in ESV supplied primarily by water bodies in UA when anthropogenic pressures increase, whereas non-UA relying on forests may experience more substantial declines. Furthermore, in contrast to UA, ES in non-UA consistently exhibit negative responses, with these adverse impacts potentially diminishing initially and subsequently intensifying. This may suggest that in non-UA, ecosystems may initially possess some resilience to mitigate adverse effects, but as anthropogenic pressures increase, ecosystems gradually deplete their resilience, leading to a progressive amplification of negative impacts. These findings underscore the critical importance of aquatic ecosystems in driving variations for urban ES.

Geographical location and economic development level influence the ES response

A comprehensive comparison of the ES response across the three UAs reveals distinct patterns. The YRD exhibits the highest sensitivity to anthropogenic pressure, followed by the MRYR, while the C&C appears relatively intricate (Fig. 5d–f). To delve deeper into these disparities, this study employed a random forest model to further analyze the internal compositional factors of anthropogenic pressure.

Firstly, the YRD, situated along the eastern coastal region of China and recognized as one of the six internationally acclaimed world-class urban agglomerations, typically boasts higher levels of economic activity, population density, and urbanization (Sun et al. 2023). These attributes could render this region more sensitive to anthropogenic pressure. Furthermore, the eastern coastal areas contend with atmospheric pollution stemming from industrial and transportation sources, further intensifying environmental stress. Secondly, the MRYR, located in central China, exhibits relatively lower levels of urbanization and economic development compared to the eastern regions (Luo et al. 2020). However, factors such as land use intensity, nighttime light index, and proximity to urban land still influence ES responses (Fig. S3). This may reflect the gradual rise in urban expansion and industrialization in central areas, subsequently elevating its response to anthropogenic pressure. Thirdly, the C&C, positioned in western China, typically experiences arid and resource-scarce conditions. Hence, ES responses might be influenced by factors such as land use and population density. However, it could also be more significantly affected by geographic, climatic, and ecosystem characteristics, such as water scarcity and ecological vulnerability. This comprehensive comparison underscores the complexity of environmental responses and sustainability in the urban agglomeration.

Policy guidelines for socio-ecological sustainability

In managing ecosystems, this study reveals the need for managers to adopt different strategies based on the diverse response patterns exhibited by different types of ecosystems. As anthropogenic pressure increases, the study identifies two main modes of ES response: one characterized by a tipping point where there is a directional shift in ES response (Fig. 6a), indicating that beyond this threshold, ES levels transition from increasing to decreasing. The other mode is characterized by a tipping point where there is a change in the magnitude of ES response (Fig. 6b), indicating that beyond this threshold, the rate of ES decline shifts from deceleration to acceleration. Based on these findings, these two modes can be distinguished to provide policy guidance for the sustainable management of ES.

Firstly, decision-makers need to recognize the spatial heterogeneity of ES responses to anthropogenic pressure, particularly in distinguishing between UA and non-UA. It is crucial to develop specific management strategies tailored to the unique characteristics of each area. Secondly, the identification and monitoring of tipping points of anthropogenic pressure are essential for effective management. It is worth noting that sustainable development goals involve not only pursuing ecological development but also achieving socio-ecological sustainability. Therefore, for Mode 1, there is a tendency to maintain the current ecological status before reaching tipping points. Once these thresholds are exceeded, proactive policies should be implemented to mitigate further degradation and restore ecosystem functionality. For Mode 2, greater priority should be given to ecological restoration, especially in areas approaching tipping points, to prevent the overall region from crossing the tipping point, as exceeding these tipping points may lead to ES collapse. In conclusion, by integrating the spatial heterogeneity of ES responses, the identification and monitoring of critical points of anthropogenic pressure, and proactive measures to prevent surpassing tipping points into policy frameworks, decision-makers can better protect and manage ecosystems, thus achieving socio-ecological sustainability at the regional level.

CONCLUSION

This study analyzed and evaluated the response of ES to anthropogenic pressure in the YREB from 2000 to 2020, yielding the following conclusions.

1. Fluctuating decline in ESV, while the increase in anthropogenic pressure: Over the past 20 years, there has been a significant negative correlation between the two.
2. Identification of a tipping point in the response of ES to anthropogenic pressure: Beyond this point, the direction or magnitude of ES change may shift, potentially leading to collapse risks, indicating a nonlinear relationship between ES and anthropogenic pressure.
3. Regional variations in ES response: Due to environmental differences, the UA exhibits characteristics of directional tipping points in ES response, while the non-UA demonstrates characteristics of magnitude tipping points. Among different UAs, the YRD shows the most intense ES response, followed by the MRYR, while the ES response in the C&C is more complex.

The nonlinear response of ES to anthropogenic pressure and its regional differences help to design effective monitoring systems and early warning mechanisms, allowing timely and targeted intervention and ensuring that resources are effectively allocated to areas of greatest need. Continuous research is vital to monitor changes, refine our understanding of ES responses under varying anthropogenic pressures, and adapt management practices accordingly. Future research will further explore the response pathways of ES to anthropogenic pressure.

Acknowledgments We would like to express our sincere gratitude to the editors and reviewers for their insightful comments and suggestions, which greatly improved the quality of this paper.

Funding This work was supported by the National Natural Science Foundation of China (Grant Numbers 42271209, 42301226), the Key Research and Development Program of Jiangxi Province (Grant Number 20223BBG71013), and the Special Funds for Water Resources in Jiangxi Province (Science and Technology Projects) (Grant Number 202425YBKT16).

REFERENCES

Banks-Leite, C., R.M. Ewers, H. Folkard-Tapp, and A. Fraser. 2020. Countering the effects of habitat loss, fragmentation, and degradation through habitat restoration. *One Earth* 3: 672–676. https://doi.org/10.1016/j.oneear.2020.11.016.

Buchadas, A., M. Baumann, P. Meyfroidt, and T. Kuemmerle. 2022. Uncovering major types of deforestation frontiers across the world's tropical dry woodlands. *Nature Sustainability* 5: 619–627. https://doi.org/10.1038/s41893-022-00886-9.

Carpenter, S.R., J.J. Cole, M.L. Pace, R. Batt, W.A. Brock, T. Cline, J. Coloso, J.R. Hodgson, et al. 2011. Early warnings of regime shifts: A whole-ecosystem experiment. *Science* 332: 1079–1082. https://doi.org/10.1126/science.1203672.

Chen, W., and G. Chi. 2022. Urbanization and ecosystem services: The multi-scale spatial spillover effects and spatial variations. *Land Use Policy* 114: 105964. https://doi.org/10.1016/j.landusepol.2021.105964.

Chen, B., X. Jing, S. Liu, J. Jiang, and Y. Wang. 2022. Intermediate human activities maximize dryland ecosystem services in the

long-term land-use change: Evidence from the Sangong River watershed, northwest China. *Journal of Environmental Management* 319: 115708. https://doi.org/10.1016/j.jenvman.2022.115708.

Chung, M.G., K.A. Frank, Y. Pokhrel, T. Dietz, and J. Liu. 2021. Natural infrastructure in sustaining global urban freshwater ecosystem services. *Nature Sustainability* 4: 1068–1075. https://doi.org/10.1038/s41893-021-00786-4.

Correa Ayram, C.A., M.E. Mendoza, A. Etter, and D.R. Pérez Salicrup. 2017. Anthropogenic impact on habitat connectivity: A multidimensional human footprint index evaluated in a highly biodiverse landscape of Mexico. *Ecological Indicators* 72: 895–909. https://doi.org/10.1016/j.ecolind.2016.09.007.

Costanza, R., R. de Groot, P. Sutton, S. van der Ploeg, S.J. Anderson, I. Kubiszewski, S. Farber, and R.K. Turner. 2014. Changes in the global value of ecosystem services. *Global Environmental Change* 26: 152–158. https://doi.org/10.1016/j.gloenvcha.2014.04.002.

Filho, L.M., P. Roebeling, S. Villasante, and M.I. Bastos. 2022. Ecosystem services values and changes across the Atlantic coastal zone: Considerations and implications. *Marine Policy* 145: 105265. https://doi.org/10.1016/j.marpol.2022.105265.

Geary, W.L., M. Bode, T.S. Doherty, E.A. Fulton, D.G. Nimmo, A.I.T. Tulloch, V.J.D. Tulloch, and E.G. Ritchie. 2020. A guide to ecosystem models and their environmental applications. *Nature Ecology and Evolution* 4: 1459–1471. https://doi.org/10.1038/s41559-020-01298-8.

Giannetti, B.F., L. Faria, C.M.V.B. Almeida, F. Agostinho, L. Coscieme, and G. Liu. 2018. Human-nature nexuses in Brazil: Monitoring production of economic and ecosystem services in historical series. *Ecosystem Services* 30: 248–256. https://doi.org/10.1016/j.ecoser.2017.10.008.

Grant, L., I. Vanderkelen, L. Gudmundsson, Z. Tan, M. Perroud, V.M. Stepanenko, A.V. Debolskiy, B. Droppers, et al. 2021. Attribution of global lake systems change to anthropogenic forcing. *Nature Geoscience* 14: 849–854. https://doi.org/10.1038/s41561-021-00833-x.

Han, R., C.-C. Feng, N. Xu, and L. Guo. 2020. Spatial heterogeneous relationship between ecosystem services and human disturbances: A case study in Chuandong, China. *Science of the Total Environment* 721: 137818. https://doi.org/10.1016/j.scitotenv.2020.137818.

IPBES. 2019. Summary for policymakers of the global assessment report on biodiversity and ecosystem services of the intergovernmental science-policy platform on biodiversity and ecosystem, ed. C.N. Zayas S. Díaz, J. Settele, E.S. Brondízio, H.T. Ngo, M. Guèze, J. Agard, A. Arneth, P. Balvanera, K.A. Brauman, S.H.M. Butchart, K.M.A. Chan, L.A. Garibaldi, K. Ichii, J. Liu, S.M. Subramanian, G.F. Midgley, P. Miloslavich, Z. Molnár, D. Obura, A. Pfa. Bonn. Germany: IPBES secretariat. https://doi.org/10.5281/zenodo.3553579.

Kéfi, S., C. Saade, E.L. Berlow, J.S. Cabral, and E.A. Fronhofer. 2022. Scaling up our understanding of tipping points. *Philosophical Transactions of the Royal Society b: Biological Sciences* 377: 1–9. https://doi.org/10.1098/rstb.2021.0386.

Keyes, A.A., J.P. McLaughlin, A.K. Barner, and L.E. Dee. 2021. An ecological network approach to predict ecosystem service vulnerability to species losses. *Nature Communications* 12: 1–11. https://doi.org/10.1038/s41467-021-21824-x.

Kong, L., T. Wu, Y. Xiao, W. Xu, X. Zhang, G.C. Daily, and Z. Ouyang. 2023. Natural capital investments in China undermined by reclamation for cropland. *Nature Ecology and Evolution* 7: 1771–1777. https://doi.org/10.1038/s41559-023-02198-3.

Li, W., L. Wang, X. Yang, T. Liang, Q. Zhang, X. Liao, J.R. White, and J. Rinklebe. 2022. Interactive influences of meteorological and socioeconomic factors on ecosystem service values in a river basin with different geomorphic features. *Science of the Total Environment* 829: 154595. https://doi.org/10.1016/j.scitotenv.2022.154595.

Lu, Y., M. Liu, S. Zeng, and C. Wang. 2021. Screening and mitigating major threats of regional development to water ecosystems using ecosystem services as endpoints. *Journal of Environmental Management* 293: 112787. https://doi.org/10.1016/j.jenvman.2021.112787.

Luo, K., and X. Zhang. 2022. Increasing urban flood risk in China over recent 40 years induced by LUCC. *Landscape and Urban Planning* 219: 104317. https://doi.org/10.1016/j.landurbplan.2021.104317.

Luo, Q., J. Zhou, Z. Li, and B. Yu. 2020. Spatial differences of ecosystem services and their driving factors: A comparation analysis among three urban agglomerations in China's Yangtze River Economic Belt. *Science of the Total Environment* 725: 138452. https://doi.org/10.1016/j.scitotenv.2020.138452.

Ma, S., L.-J. Wang, J. Jiang, and Y.-G. Zhao. 2023. Direct and indirect effects of agricultural expansion and landscape fragmentation processes on natural habitats. *Agriculture, Ecosystems and Environment* 353: 108555. https://doi.org/10.1016/j.agee.2023.108555.

Maestre, F.T., Y. Le Bagousse-Pinguet, M. Delgado-Baquerizo, D.J. Eldridge, H. Saiz, M. Berdugo, B. Gozalo, V. Ochoa, et al. 2022. Grazing and ecosystem service delivery in global drylands. *Science* 378: 915–920. https://doi.org/10.1126/science.abq4062.

Marques, A., I.S. Martins, T. Kastner, C. Plutzar, M.C. Theurl, N. Eisenmenger, M.A.J. Huijbregts, R. Wood, et al. 2019. Increasing impacts of land use on biodiversity and carbon sequestration driven by population and economic growth. *Nature Ecology and Evolution* 3: 628–637. https://doi.org/10.1038/s41559-019-0824-3.

Mumby, P.J., A. Hastings, and H.J. Edwards. 2007. Thresholds and the resilience of Caribbean coral reefs. *Nature* 450: 98–101. https://doi.org/10.1038/nature06252.

Nava, V., S. Chandra, J. Aherne, M.B. Alfonso, A.M. Antão-Geraldes, K. Attermeyer, R. Bao, M. Bartrons, et al. 2023. Plastic debris in lakes and reservoirs. *Nature* 619: 317–322. https://doi.org/10.1038/s41586-023-06168-4.

Nijhum, F., C. Westbrook, B. Noble, K. Belcher, and P. Lloyd-Smith. 2021. Evaluation of alternative land-use scenarios using an ecosystem services-based strategic environmental assessment approach. *Land Use Policy* 108: 105540. https://doi.org/10.1016/j.landusepol.2021.105540.

Pan, Y., F. Dong, and C. Du. 2023. Is China approaching the inflection point of the ecological Kuznets curve? Analysis based on ecosystem service value at the county level. *Journal of Environmental Management* 326: 116629. https://doi.org/10.1016/j.jenvman.2022.116629.

Peng, K., W. Jiang, Z. Ling, P. Hou, and Y. Deng. 2021. Evaluating the potential impacts of land use changes on ecosystem service value under multiple scenarios in support of SDG reporting: A case study of the Wuhan urban agglomeration. *Journal of Cleaner Production* 307: 127321. https://doi.org/10.1016/j.jclepro.2021.127321.

Pham, K.T., and T.-H. Lin. 2023. Effects of urbanisation on ecosystem service values: A case study of Nha Trang, Vietnam. *Land Use Policy* 128: 106599. https://doi.org/10.1016/j.landusepol.2023.106599.

Pires de Souza Araujo, A.C., D. Souza dos Santos, F. Lins-de-Barros, and S. de Souza Hacon. 2021. Linking ecosystem services and human health in coastal urban planning by DPSIWR framework. *Ocean and Coastal Management* 210: 105728. https://doi.org/10.1016/j.ocecoaman.2021.105728.

Qi, Y., X. Lian, H. Wang, J. Zhang, and R. Yang. 2020. Dynamic mechanism between human activities and ecosystem services: A

case study of Qinghai lake watershed, China. *Ecological Indicators* 117: 106528. https://doi.org/10.1016/j.ecolind.2020.106528.

Sanderson, E.W., M. Jaiteh, M.A. Levy, K.H. Redford, A.V. Wannebo, and G. Woolmer. 2002. The human footprint and the last of the wild: The human footprint is a global map of human influence on the land surface, which suggests that human beings are stewards of nature, whether we like it or not. *BioScience* 52: 891–904. https://doi.org/10.1641/0006-3568(2002)052[0891:THFATL]2.0.CO.

Scheffer, M., S. Carpenter, J.A. Foley, C. Folke, and B. Walker. 2001. Catastrophic shifts in ecosystems. *Nature* 413: 591–596. https://doi.org/10.1038/35098000.

Shi, J., S. Li, Y. Song, N. Zhou, K. Guo, and J. Bai. 2022. How socioeconomic factors affect ecosystem service value: Evidence from China. *Ecological Indicators* 145: 109589. https://doi.org/10.1016/j.ecolind.2022.109589.

Smith, K.E., M.T. Burrows, A.J. Hobday, A. Sen Gupta, P.J. Moore, M. Thomsen, T. Wernberg, and D.A. Smale. 2022. Socioeconomic impacts of marine heatwaves: Global issues and opportunities. *Science* 374: eabj3593. https://doi.org/10.1126/science.abj3593.

Souza, B.A., J.C.S. Rosa, J. Siqueira-Gay, and L.E. Sánchez. 2021. Mitigating impacts on ecosystem services requires more than biodiversity offsets. *Land Use Policy* 105: 105393. https://doi.org/10.1016/j.landusepol.2021.105393.

Sun, B., C. Fang, X. Liao, X. Guo, and Z. Liu. 2023. The relationship between urbanization and air pollution affected by intercity factor mobility: A case of the Yangtze River Delta region. *Environmental Impact Assessment Review* 100: 107092. https://doi.org/10.1016/j.eiar.2023.107092.

Thaweepworadej, P., and K.L. Evans. 2022. Avian species richness and tropical urbanization gradients: Effects of woodland retention and human disturbance. *Ecological Applications* 32: e2586. https://doi.org/10.1002/eap.2586.

Theobald, D.M. 2013. A general model to quantify ecological integrity for landscape assessments and US application. *Landscape Ecology* 28: 1859–1874. https://doi.org/10.1007/s10980-013-9941-6.

van Belzen, J., J. van de Koppel, M.L. Kirwan, D. van der Wal, P.M.J. Herman, V. Dakos, S. Kéfi, M. Scheffer, et al. 2017. Vegetation recovery in tidal marshes reveals critical slowing down under increased inundation. *Nature Communications* 8: 15811. https://doi.org/10.1038/ncomms15811.

Venter, O., E.W. Sanderson, A. Magrach, J.R. Allan, J. Beher, K.R. Jones, H.P. Possingham, W.F. Laurance, et al. 2016. Sixteen years of change in the global terrestrial human footprint and implications for biodiversity conservation. *Nature Communications* 7: 12558. https://doi.org/10.1038/ncomms12558.

Wan, J., C. Wang, and F. Yu. 2018. Human footprint and climate disappearance in vulnerable ecoregions of protected areas. *Global and Planetary Change* 170: 260–268. https://doi.org/10.1016/j.gloplacha.2018.09.002.

Wang, C., L. Wang, J. Zhan, W. Liu, Y. Teng, X. Chu, and H. Wang. 2022. Spatial heterogeneity of urbanization impacts on ecosystem services in the urban agglomerations along the Yellow River, China. *Ecological Engineering* 182: 106717. https://doi.org/10.1016/j.ecoleng.2022.106717.

Wang, Z., H. Zhou, X. Wang, and Y. Shang. 2021. *Annual report on the development of Yangtze River Economic Belt*. Beijing: Social Science Academic Press (in Chinese).

Xie, G., C. Zhang, L. Zhang, W. Chen, and M. Shi. 2015. Improvement of the evaluation method for ecosystem service value based on per unit area. *Journal of Natural Resources* 30: 1243–1254. https://doi.org/10.11849/zrzyxb.2015.08.001. (in Chinese).

Yang, Q., G. Liu, M. Casazza, S. Dumontet, and Z. Yang. 2022a. Ecosystem restoration programs challenges under climate and land use change. *Science of the Total Environment* 807: 150527. https://doi.org/10.1016/j.scitotenv.2021.150527.

Yang, R., F. Ren, W. Xu, X. Ma, H. Zhang, and W. He. 2022b. China's ecosystem service value in 1992–2018: Pattern and anthropogenic driving factors detection using Bayesian spatiotemporal hierarchy model. *Journal of Environmental Management* 302: 114089. https://doi.org/10.1016/j.jenvman.2021.114089.

Yongxiu, S., L. Shiliang, S. Fangning, A. Yi, L. Mingqi, and L. Yixuan. 2020. Spatio-temporal variations and coupling of human activity intensity and ecosystem services based on the four-quadrant model on the Qinghai-Tibet Plateau. *Science of the Total Environment* 743: 140721. https://doi.org/10.1016/j.scitotenv.2020.140721.

Yu, P., S. Zhang, E.H.K. Yung, E.H.W. Chan, B. Luan, and Y. Chen. 2023. On the urban compactness to ecosystem services in a rapidly urbanising metropolitan area: Highlighting scale effects and spatial non-stationary. *Environmental Impact Assessment Review* 98: 106975. https://doi.org/10.1016/j.eiar.2022.106975.

Zalles, V., M.C. Hansen, P.V. Potapov, D. Parker, S.V. Stehman, A.H. Pickens, L.L. Parente, L.G. Ferreira, et al. 2023. Rapid expansion of human impact on natural land in South America since 1985. *Science Advances* 7: eabg1620. https://doi.org/10.1126/sciadv.abg1620.

Zhang, Z., J. Peng, Z. Xu, X. Wang, and J. Meersmans. 2021. Ecosystem services supply and demand response to urbanization: A case study of the Pearl River Delta, China. *Ecosystem Services* 49: 101274. https://doi.org/10.1016/j.ecoser.2021.101274.

Zhu, W., Y. Pan, H. Hu, J. Li, and P. Gong. 2005. Estimating net primary productivity of terrestrial vegetation based on remote sensing: A case study in Inner Mongolia, China. *Journal of Remote Sensing* 3: 300–307. https://doi.org/10.1109/IGARSS.2004.1369080.

AUTHOR BIOGRAPHIES

Chenghao Liu is a doctoral candidate at the Nanchang University. Her research interests include ecosystem services and coupling of human activities and ecosystems.
Address: School of Economics and Management, Nanchang University, 999 Xuefu Road, Nanchang 330031, Jiangxi, People's Republic of China.
e-mail: chliu@email.ncu.edu.cn

Yaobin Liu (✉) is a Professor at the Nanchang University. His research interests include ecological economics and environmental economics.
Address: School of Economics and Management, Nanchang University, 999 Xuefu Road, Nanchang 330031, Jiangxi, People's Republic of China.
Address: Key Laboratory of Poyang Lake Environment and Resource Utilization, Ministry of Education, School of Resource and

Environment, Nanchang University, Nanchang 330031, People's Republic of China.
e-mail: liuyaobin@ncu.edu.cn

Biagio Fernando Giannetti is a Professor at the Paulista University. His research interests include environmental assessment, cleaner production, and sustainable development.
Address: Laboratory of Production and Environment, Universidade Paulista, R. Dr Bacelar, 1212, São Paulo 04026-002, Brazil.
e-mail: biafgian@unip.br

Cecília Maria Villas Bôas de Almeida is a Professor at the Paulista University. Her research interests include environmental assessment, cleaner production, and sustainable development.
Address: Laboratory of Production and Environment, Universidade Paulista, R. Dr Bacelar, 1212, São Paulo 04026-002, Brazil.
e-mail: cmvbag@unip.br

Guoen Wei is a postdoctoral fellow at the Nanchang University. His research interests include land use changes and environmental assessment.
Address: School of Resources and Environment, Nanchang University, 999 Xuefu Road, Honggutan District, Nanchang 330031, Jiangxi, People's Republic of China.
e-mail: weiguoen22@ncu.edu.cn

Fábio Sevegnani is a Professor at the Paulista University. His research interests include environmental assessment, cleaner production, and sustainable development.
Address: Laboratory of Production and Environment, Universidade Paulista, R. Dr Bacelar, 1212, São Paulo 04026-002, Brazil.
e-mail: fabio.sevegnani@docente.unip.br

Xiaolu Yan is an Associate Professor at the Liaoning Normal University. Her research interests include blue carbon and landscape ecology.
Address: Key Research Base of Humanities and Social Sciences of Ministry of Education, Institute of Marine Sustainable Development, Liaoning Normal University, 850 Huanghe Road, Shahekou District, Dalian 116029, Liaoning, People's Republic of China.
e-mail: xlyan@lnnu.edu.cn